

# DC-DC Power Converters

Robert W. Erickson

Department of Electrical and Computer Engineering

University of Colorado

Boulder, CO 80309-0425

Dc-dc power converters are employed in a variety of applications, including power supplies for personal computers, office equipment, spacecraft power systems, laptop computers, and telecommunications equipment, as well as dc motor drives. The input to a dc-dc converter is an unregulated dc voltage  $V_g$ . The converter produces a regulated output voltage  $V$ , having a magnitude (and possibly polarity) that differs from  $V_g$ . For example, in a computer off-line power supply, the 120 V or 240 V ac utility voltage is rectified, producing a dc voltage of approximately 170 V or 340 V, respectively. A dc-dc converter then reduces the voltage to the regulated 5 V or 3.3 V required by the processor ICs.

High efficiency is invariably required, since cooling of inefficient power converters is difficult and expensive. The ideal dc-dc converter exhibits 100% efficiency; in practice, efficiencies of 70% to 95% are typically obtained. This is achieved using *switched-mode*, or *chopper*,

circuits whose elements dissipate negligible power. *Pulse-width modulation* (PWM) allows control and regulation of the total output voltage. This approach is also employed in applications involving alternating current, including high-efficiency dc-ac power converters (inverters and power amplifiers), ac-ac power converters, and some ac-dc power converters (low-harmonic rectifiers).

A basic dc-dc converter circuit known as the *buck converter* is illustrated in Fig. 1. A single-pole double-throw (SPDT) switch is connected to the dc input voltage  $V_g$  as shown. The switch output voltage

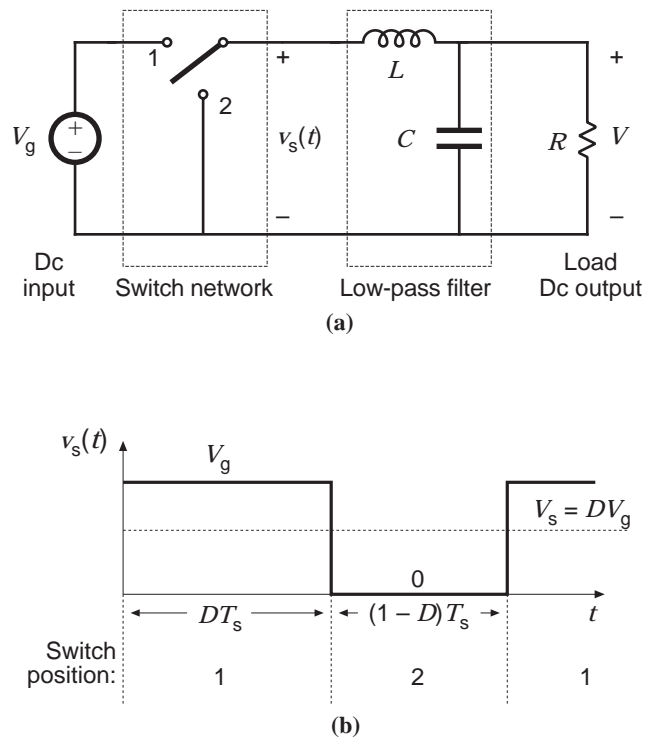


**Figure 1.** The buck converter consists of a switch network that reduces the dc component of voltage, and a low-pass filter that removes the high-frequency switching harmonics: (a) schematic, (b) switch voltage waveform.

$v_s(t)$  is equal to  $V_g$  when the switch is in position 1, and is equal to zero when the switch is in position 2. The switch position varies periodically, such that  $v_s(t)$  is a rectangular waveform having period  $T_s$  and duty cycle  $D$ . The duty cycle is equal to the fraction of time that the switch is connected in position 1, and hence  $0 \leq D \leq 1$ . The *switching frequency*  $f_s$  is equal to  $1/T_s$ . In practice, the SPDT switch is realized using semiconductor devices such as diodes, power MOSFETs, IGBTs, BJTs, or thyristors. Typical switching frequencies lie in the range 1 kHz to 1 MHz, depending on the speed of the semiconductor devices.

The switch network changes the dc component of the voltage. By Fourier analysis, the dc component of a waveform is given by its average value. The average value of  $v_s(t)$  is given by

$$V_s = \frac{1}{T_s} \int_0^{T_s} v_s(t) dt = DV_g \quad (1)$$

The integral is equal to the area under the waveform, or the height  $V_g$  multiplied by the time  $DT_s$ . It can be seen that the switch network reduces the dc component of the voltage by a factor equal to the duty cycle  $D$ . Since  $0 \leq D \leq 1$ , the dc component of  $V_s$  is less than or equal to  $V_g$ .

The power dissipated by the switch network is ideally equal to zero. When the switch contacts are closed, then the voltage across the contacts is equal to zero and hence the power dissipation is zero. When the switch contacts are open, then there is zero current and the power dissipation is again equal to zero. Therefore, the ideal switch network is able to change the dc component of voltage without dissipation of power.

In addition to the desired dc voltage component  $V_s$ , the switch waveform  $v_s(t)$  also contains undesired harmonics of the switching frequency. In most applications, these harmonics must be removed, such that the converter output voltage  $v(t)$  is essentially equal to the dc component  $V = V_s$ . A low-pass filter is employed for this purpose. The converter of Fig. 1 contains a single-section  $L$ - $C$  low-pass filter. The filter has corner frequency  $f_0$  given by

$$f_0 = \frac{1}{2\pi\sqrt{LC}} \quad (2)$$

The corner frequency  $f_0$  is chosen to be sufficiently less than the switching frequency  $f_s$ , so that the filter essentially passes only the dc component of  $v_s(t)$ . To the extent that the inductor and capacitor are ideal, the filter removes the switching harmonics without dissipation of power. Thus, the converter produces a dc output voltage whose magnitude is controllable via the duty cycle  $D$ , using circuit elements that (ideally) do not dissipate power.

The *conversion ratio*  $M(D)$  is defined as the ratio of the dc output voltage  $V$  to the dc input voltage  $V_g$  under steady-state conditions:

$$M(D) = \frac{V}{V_g} \quad (3)$$

For the buck converter,  $M(D)$  is given by

$$M(D) = D \quad (4)$$

This equation is plotted in Fig. 2. It can be seen that the dc output voltage  $V$  is controllable between 0 and  $V_g$ , by adjustment of the duty cycle  $D$ .

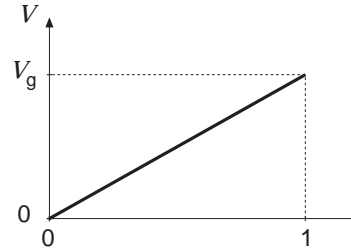


**Figure 2.** Buck converter dc output voltage  $V$  vs. duty cycle  $D$ .

Figure 3 illustrates one way to realize the switch network in the buck converter, using a power MOSFET and diode. A gate drive circuit switches the MOSFET between the conducting (on) and blocking (off) states, as commanded by a logic signal  $\delta(t)$ . When  $\delta(t)$  is high (for  $0 < t < DT_s$ ), then MOSFET  $Q_1$  conducts with negligible drain-to-source voltage. Hence,  $v_s(t)$  is approximately equal to  $V_g$ , and the diode is reverse-biased. The positive inductor current  $i_L(t)$  flows through the MOSFET. At time  $t = DT_s$ ,  $\delta(t)$  becomes low, commanding MOSFET  $Q_1$  to turn off. The inductor current must continue to flow; hence,  $i_L(t)$  forward-biases diode  $D_1$ , and  $v_s(t)$  is now approximately equal to zero. Provided that the inductor current  $i_L(t)$  remains positive, then diode  $D_1$  conducts for the remainder of the switching period. Diodes that operate in the manner are called *freewheeling diodes*.

Since the converter output voltage  $v(t)$  is a function of the switch duty cycle  $D$ , a control system can be constructed that varies the duty cycle to cause the output voltage to follow a given reference  $v_r$ . Figure 3 illustrates the block diagram of a simple converter feedback system. The output voltage is sensed using a voltage divider, and is compared with an accurate dc reference voltage  $v_r$ . The resulting error signal is passed through an op-amp compensation

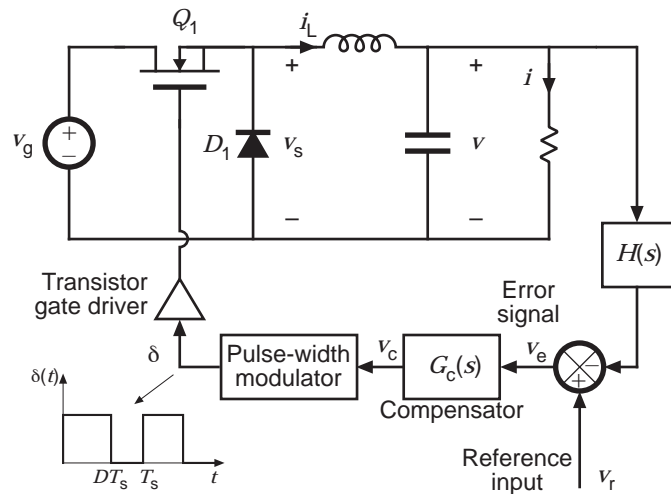


**Figure 3.** Realization of the ideal SPDT switch using a transistor and freewheeling diode. In addition, a feedback loop is added for regulation of the output voltage.

network. The analog voltage  $v_c(t)$  is next fed into a *pulse-width modulator*. The modulator produces a switched voltage waveform that controls the gate of the power MOSFET  $Q_1$ . The duty cycle  $D$  of this waveform is proportional to the control voltage  $v_c(t)$ . If this control system is well designed, then the duty cycle is automatically adjusted such that the converter output voltage  $v$  follows the reference voltage  $v_r$ , and is essentially independent of variations in  $v_g$  or load current.

## Converter circuit topologies

A large number of dc-dc converter circuits are known that can increase or decrease the magnitude of the dc voltage and/or invert its polarity [1-5]. Figure 4 illustrates several commonly used dc-dc converter circuits, along with their respective conversion ratios. In each example, the switch is realized using a power MOSFET and diode; however, other semiconductor switches such as IGBTs, BJTs, or thyristors can be substituted if desired.

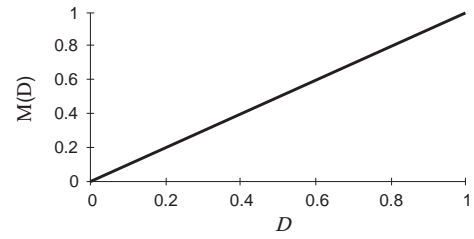
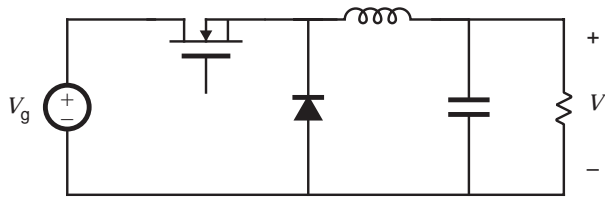
The first converter is the buck converter, which reduces the dc voltage and has conversion ratio  $M(D) = D$ . In a similar topology known as the boost converter, the positions of the switch and inductor are interchanged. This converter produces an output voltage  $V$  that is greater in magnitude than the input voltage  $V_g$ . Its conversion ratio is  $M(D) = 1/(1 - D)$ .

In the buck-boost converter, the switch alternately connects the inductor across the power input and output voltages. This converter inverts the polarity of the voltage, and can either increase or decrease the voltage magnitude. The conversion ratio is  $M(D) = -D/(1 - D)$ .

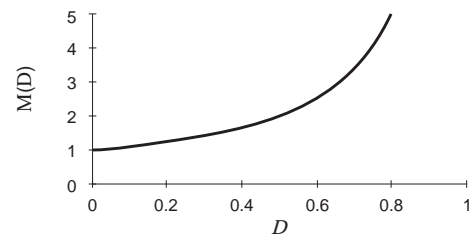
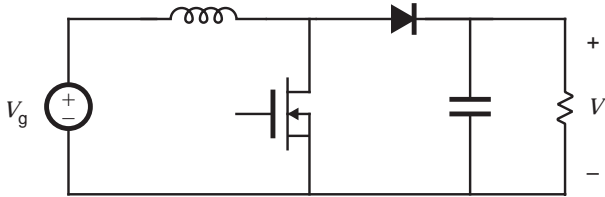
The Cuk converter contains inductors in series with the converter input and output ports. The switch network alternately connects a capacitor to the input and output inductors. The conversion ratio  $M(D)$  is identical to that of the buck-boost converter. Hence, this converter also inverts the voltage polarity, while either increasing or decreasing the voltage magnitude.

The single-ended primary inductance converter (SEPIC) can also either increase or decrease the voltage magnitude. However, it does not invert the polarity. The conversion ratio is  $M(D) = D/(1 - D)$ .

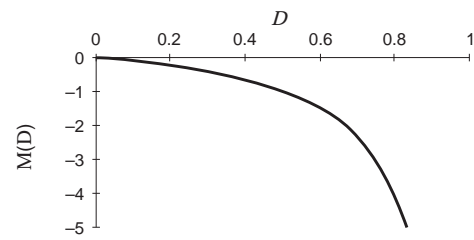
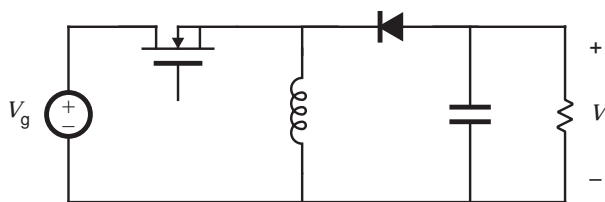
Buck converter



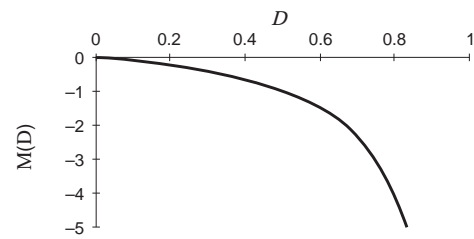
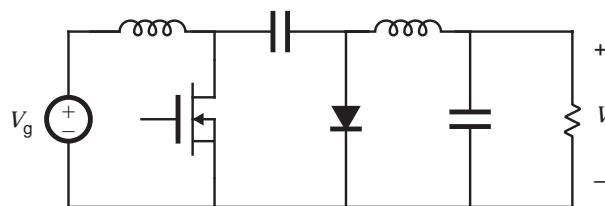
Boost converter



Buck-boost converter



Cuk converter



SEPIC

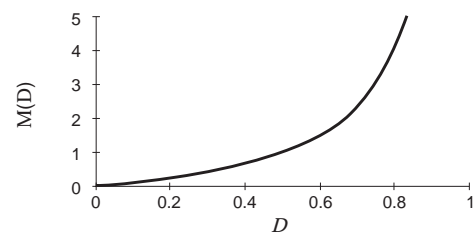
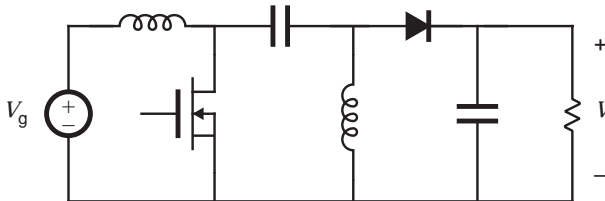


Figure 4. Several basic dc-dc converters and their dc conversion ratios  $M(D) = V/V_g$ .

## Analysis of converter waveforms

Under steady-state conditions, the voltage and current waveforms of a dc-dc converter can be found by use of two basic circuit analysis principles. The principle of *inductor volt-second balance* states that the average value, or dc component, of voltage applied across an ideal inductor winding must be zero. This principle also applies to each winding of a transformer or other multiple winding magnetic devices. Its dual, the principle of *capacitor amp-second* or *charge balance*, states that the average current that flows through an ideal capacitor must be zero. Hence, to determine the voltages and currents of dc-dc converters operating in periodic steady state, one averages the inductor current and capacitor voltage waveforms over one switching period, and equates the results to zero.

The equations are greatly simplified by use of a third artifice, the *small ripple approximation*. The inductor currents and capacitor voltages contain dc components, plus *switching ripple* at the switching frequency and its harmonics. In most well designed converters, the switching ripple is small in magnitude compared to the dc components. For inductor currents, a typical value of switching ripple at maximum load is 10% to 20% of the dc component of current. For an output capacitor voltage, the switching ripple is typically required to be much less than 1% of the dc output voltage. In both cases, the ripple magnitude is small compared with the dc component, and can be ignored.

As an example, consider the boost converter of Fig. 5(a). A resistor  $R_L$  is included in series with the inductor, to model the resistance of the inductor winding. It is desired to determine simple expressions for the output voltage  $V$ , inductor current  $I_L$ , and efficiency  $\eta$ . Typical inductor voltage and capacitor current waveforms are sketched in Fig. 5(b).

With the switch in position 1, the inductor voltage is equal to  $v_L(t) = V_g - i_L(t)R_L$ . By use of the small ripple approximation, we can replace  $i_L(t)$  with its dc component  $I_L$ , and hence obtain  $v_L(t) \approx V_g - I_L R_L$ . Likewise, the capacitor current is equal to  $i_C(t) = -v(t)/R$ , which can be approximated as  $i_C(t) \approx -V/R$ .

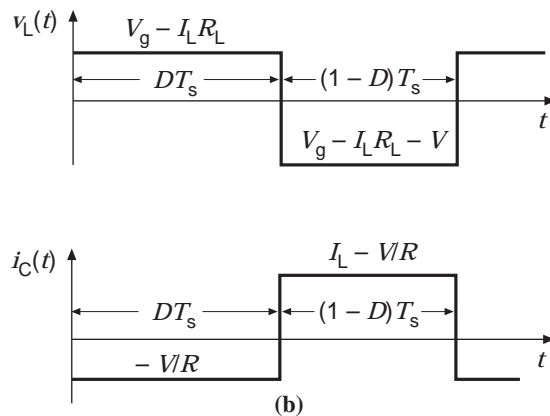
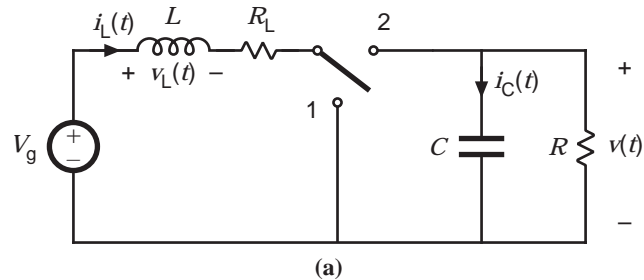


**Figure 5.** A nonideal boost converter: (a) schematic, (b) inductor voltage and capacitor current waveforms.

When the switch is in position 2, the inductor is connected between the input and output voltages. The inductor voltage can now be written  $v_L(t) = V_g - i_L(t)R_L - v(t) \approx V_g - I_L R_L - V$ . The capacitor current can be expressed as  $i_C(t) = i_L(t) - v(t)/R \approx I_L - V/R$ .

When the converter operates in steady state, the average value, or dc component, of the inductor voltage waveform  $v_L(t)$  must be equal to zero. Upon equating the average value of the  $v_L(t)$  waveform of Fig. 5(b) to zero, we obtain

$$0 = D(V_g - I_L R_L) + (1 - D)(V_g - I_L R_L - V) \quad (5)$$

Likewise, application of the principle of capacitor charge balance to the capacitor current waveform of Fig. 5(b) leads to

$$0 = D\left(-\frac{V}{R}\right) + (1 - D)\left(I - \frac{V}{R}\right) \quad (6)$$

Equations (5) and (6) can now be solved for the unknowns  $V$  and  $I_L$ . The result is

$$\frac{V}{V_g} = \frac{1}{(1 - D)} \frac{1}{\left(1 + \frac{R_L}{(1 - D)^2 R}\right)} \quad (7)$$

$$I_L = \frac{V_g}{(1 - D)^2 R} \frac{1}{\left(1 + \frac{R_L}{(1 - D)^2 R}\right)} \quad (8)$$

Equation (7) is plotted in Fig. 6, for several values of  $R_L/R$ . In the ideal case when  $R_L = 0$ , the voltage conversion ratio  $M(D)$  is equal to one at  $D = 0$ , and tends to infinity as  $D$  approaches one. In the practical case where some small inductor resistance  $R_L$  is present, the output voltage tends to zero at  $D = 1$ . In addition, it can be seen that the inductor winding resistance  $R_L$  (and other loss elements as well) limits the maximum output voltage that the converter can produce. Obtaining a given large value of  $V/V_g$  requires that the winding resistance  $R_L$  be sufficiently small.

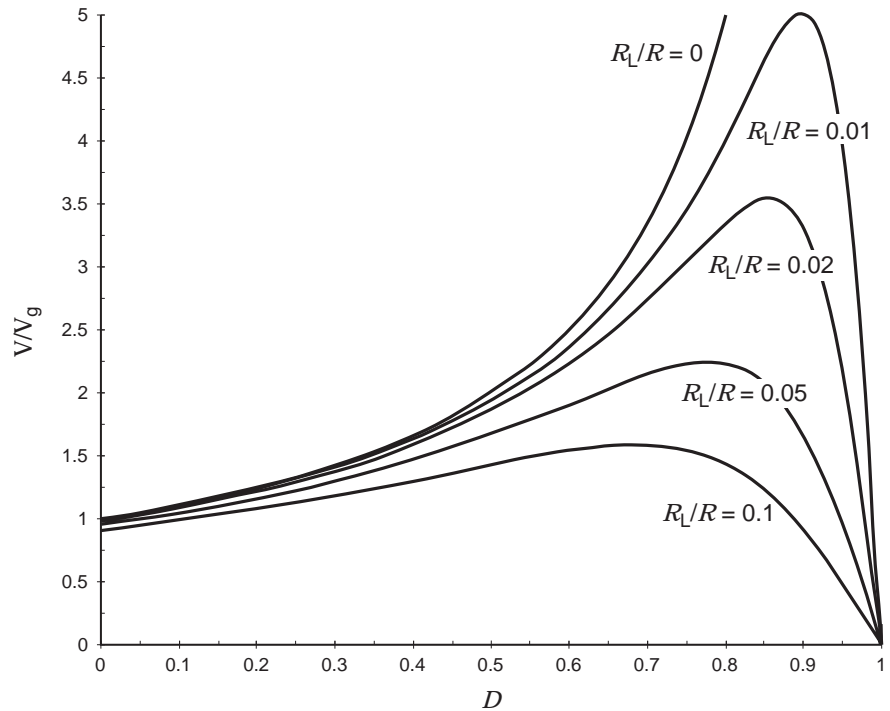


**Figure 6.** Output voltage vs. duty cycle, for the nonideal boost converter of Fig. 5.

The converter efficiency can also be determined. For this boost converter example, the efficiency is equal to

$$\eta = \frac{P_{\text{out}}}{P_{\text{in}}} = \frac{(V^2/R)}{(V_g I_L)} \quad (9)$$

Substitution of Eqs. (7) and (8) into Eq. (9) leads to

$$\eta = \frac{1}{\left(1 + \frac{R_L}{(1-D)^2 R}\right)} \quad (10)$$

This expression is plotted in Fig. 7, again for several values of  $R_L/R$ . It can be seen that, to obtain high efficiency, the inductor winding resistance  $R_L$  should be much smaller than  $(1-D)^2 R$ . This is much easier to accomplish at low duty cycles, where  $(1-D)$  is close to unity, that at high duty cycles where

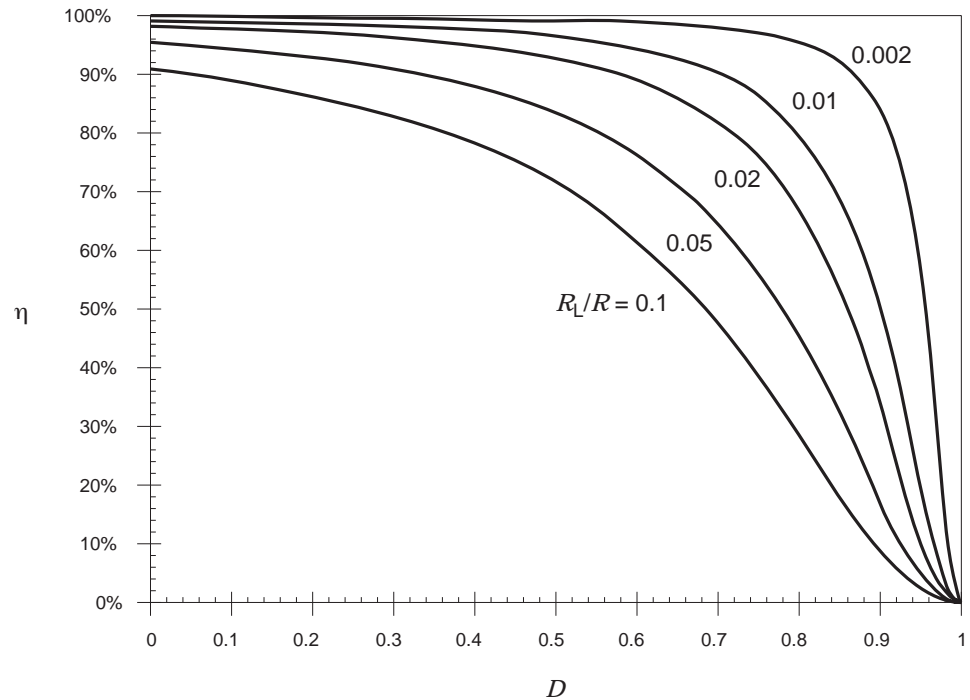


Figure 7. Efficiency vs. duty cycle, for the nonideal boost converter of Fig. 5.

$(1-D)$  approaches zero. Consequently, the efficiency is high at low duty cycles, but decreases rapidly to zero near  $D = 1$ . This behavior is typical of converters having boost or buck-boost characteristics.

## Transformer isolation

In the majority of applications, it is desired to incorporate a transformer into the switching converter, to obtain dc isolation between the converter input and output. For example, in off-line power supply applications, isolation is usually required by regulatory agencies. This isolation could be obtained by simply connecting a 50 Hz or 60 Hz transformer at the power supply ac input terminals. However, since transformer size and weight vary inversely with frequency, incorporation of the transformer into the converter can make significant improvements: the transformer then operates at the converter switching frequency of tens or hundreds of kilohertz. The size of modern ferrite power transformers is minimized at

operating frequencies ranging from several hundred kilohertz to roughly one Megahertz. These high frequencies lead to dramatic reductions in transformer size.

When a large step-up or step-down conversion ratio is required, the use of a transformer can allow better converter optimization. By proper choice of the transformer turns ratio, the voltage or current stresses imposed on the transistors and diodes can be minimized, leading to improved efficiency and lower cost.

Multiple dc outputs can also be obtained in an inexpensive manner, by adding multiple secondary windings and converter secondary-side circuits. The secondary turns ratios are chosen to obtain the desired output voltages. Usually, only one output voltage can be regulated, via control of the converter duty cycle, so wider tolerances must be allowed for the auxiliary output voltages. *Cross regulation* is a measure of the variation in an auxiliary output voltage, given that the main output voltage is regulated perfectly.

The basic operation of transformers in most power converters can be understood by replacing the transformer with the simplified model illustrated in Fig. 8. The model neglects losses and imperfect coupling between windings; such phenomena are usually considered to be converter nonidealities. The model consists of an ideal transformer plus a shunt inductor known as the magnetizing inductance  $L_M$ . This inductor models the magnetization of the physical transformer core, and hence it must obey all of the usual rules for inductors. In particular, volt-second balance must be maintained on the magnetizing inductance. Furthermore, since the voltages of all windings of the ideal transformer are proportional, volt-second balance must be maintained for each winding. Failure to achieve volt-second balance leads to transformer saturation and, usually, destruction of the converter. The means by which transformer volt-second balance is achieved is known as the *transformer reset* mechanism.

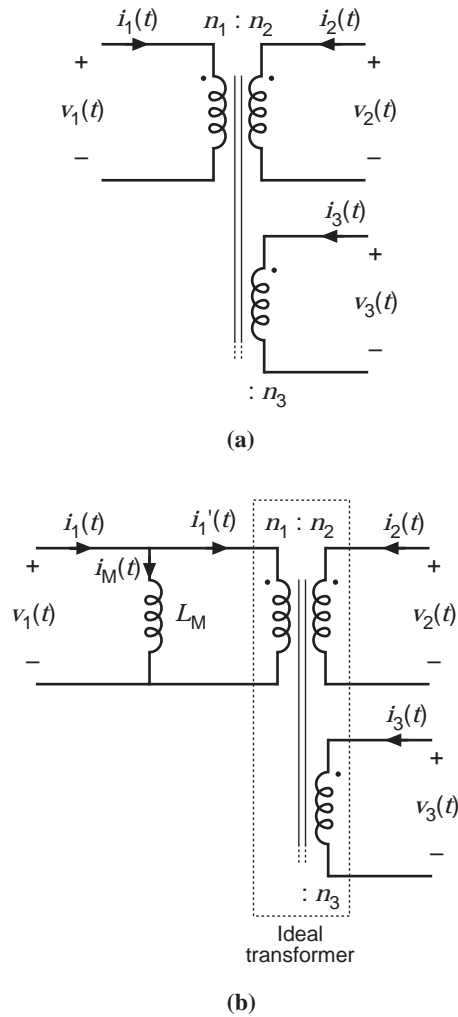


**Figure 8.** Modeling a physical transformer such that its basic operation within an isolated dc-dc converter can be understood: (a) transformer schematic symbol, (b) equivalent circuit model that includes magnetizing inductance  $L_M$  and an ideal transformer.

There are several ways of incorporating transformer isolation into any dc-dc converter. The full-bridge, half-bridge, forward, and push-pull converters are commonly used isolated versions of the buck converter. Similar isolated variants of the boost converter are known. The flyback converter is an isolated version of the buck-boost converter. Isolated variants of the SEPIC and Cuk converter are also known. The full-bridge, forward, and flyback converters are briefly described in this section.

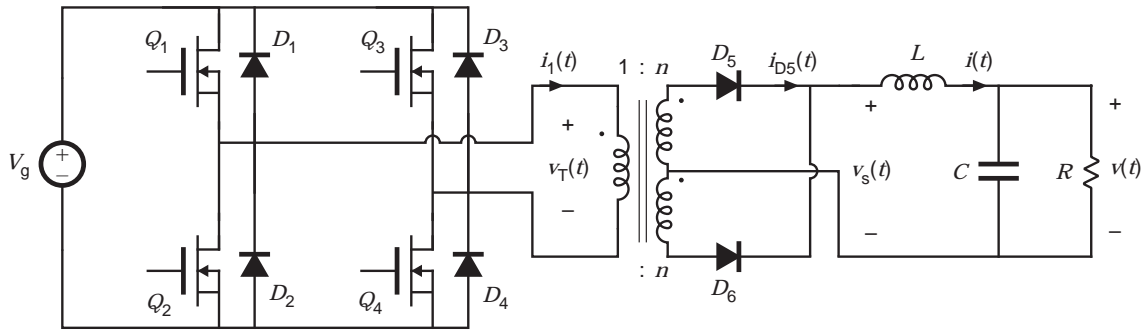


Figure 9. The full bridge transformer-isolated buck converter.

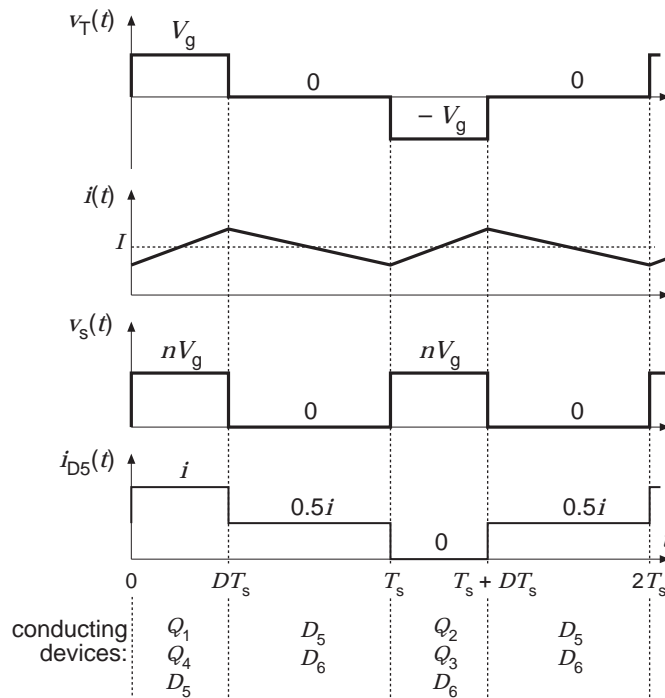


Figure 10. Waveforms of the full bridge circuit of Fig. 9.

### Full-bridge buck-derived converter

The full-bridge transformer-isolated buck converter is sketched in Fig. 9. Typical waveforms are illustrated in Fig. 10.

The transformer primary winding is driven symmetrically, such that the net volt-seconds applied over two switching periods is equal to zero. During the first switching period, transistors  $Q_1$  and  $Q_4$  conduct

for time  $DT_s$ . The volt-seconds applied to the primary winding during this switching period are equal to  $V_gDT_s$ . During the following switching period, transistors  $Q_2$  and  $Q_3$  conduct for time  $DT_s$ , thereby applying  $-V_gDT_s$  volt-seconds to the transformer primary winding. Over two switching periods, the net applied volt-seconds is equal to zero.

In practice, there exist small imbalances such as the small differences in the transistor forward voltage drops or transistor switching times, so that the average primary winding voltage is small but nonzero. This nonzero dc voltage can lead to transformer saturation and destruction of the converter. Transformer saturation under steady state conditions can be avoided by placing a capacitor in series with the transformer primary. Imbalances then induce a dc voltage component across the capacitor, rather than across the transformer primary. Another solution is the use of current programmed control; the series capacitor is then omitted.

By application of the principle of volt-second balance to the output filter inductor voltage, the dc load voltage can be shown to be

$$V = nDV_g \quad (11)$$

So, as in the buck converter, the output voltage can be controlled by adjustment of the transistor duty cycle  $D$ . An additional increase or decrease of the voltage  $V$  can be obtained via the physical transformer turns ratio  $n$ .

The full bridge configuration is typically used in switching power supplies at power levels of approximately 750 W or greater. At lower power levels, approaches such as the forward converter are preferred because of their lower parts count. Four transistors and their associated drive circuits are required. The utilization of the transformer is good, leading to small transformer size. The transformer operating frequency is one-half of the transistor switching frequency.

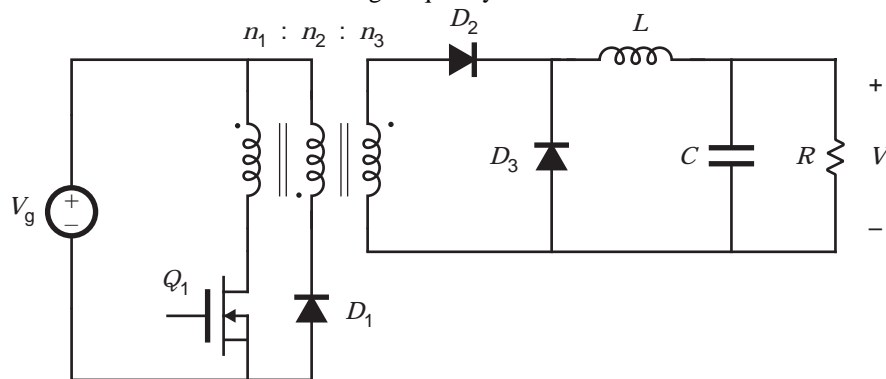


**Figure 11.** The forward converter, a single-transistor isolated buck converter.

### ***Forward converter***

The forward converter is illustrated in Fig. 11. This transformer-isolated converter is also based on the buck converter. It requires a single transistor, and therefore finds application at power levels lower than

those encountered in the full bridge circuit. The maximum transistor duty cycle is limited in value; for the common choice  $n_1 = n_2$ , the duty cycle is limited to the range  $D < 0.5$ .

The transformer is reset while transistor  $Q_1$  is in the off state. While the transistor conducts, the input voltage  $V_g$  is applied across the transformer primary winding. This causes the transformer magnetizing current to increase. When transistor  $Q_1$  turns off, the transformer magnetizing current forward-biases diode  $D_1$ , and hence voltage  $-V_g$  is applied to the second winding. This negative voltage causes the magnetizing current to decrease. When the magnetizing current reaches zero, diode  $D_1$  turns off. Volt-second balance is maintained on the transformer windings provided that the magnetizing current reaches zero before the end of the switching period. It can be shown that this occurs when

$$D \leq \frac{1}{1 + \frac{n_2}{n_1}} \quad (12)$$

For the common choice  $n_2 = n_1$ , this expression reduces to

$$D \leq \frac{1}{2} \quad (13)$$

Hence, the maximum duty cycle is limited. If this limit is violated, then the transistor off time is insufficient to reset the transformer. There will then be a net increase in the transformer magnetizing current over each switching period, and the transformer will eventually saturate.

The converter output voltage can be found by application of the principle of inductor volt-second balance to the output filter inductor  $L$ . The result is

$$V = \frac{n_3}{n_1} DV_g \quad (14)$$

This expression is subject to the constraint given in Eq. (12).

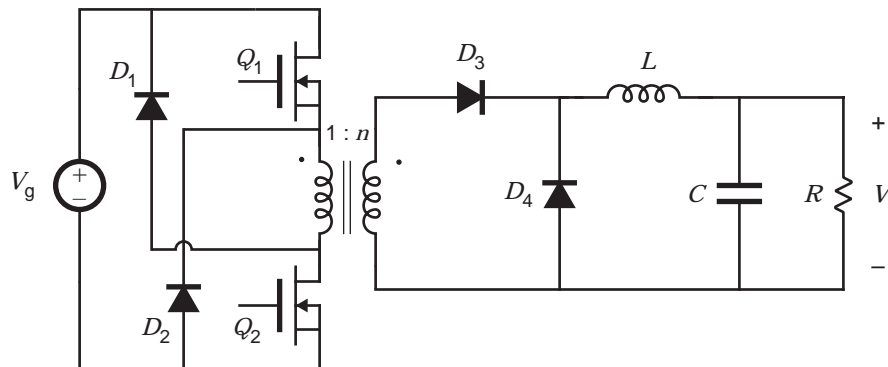


**Figure 12.** A two-transistor version of the forward converter.

A two-transistor version of the forward converter is illustrated in Fig. 12. Transistors  $Q_1$  and  $Q_2$  are controlled by the same gate drive signal, such that they conduct simultaneously. After the transistors turn off, the transformer magnetizing current forward-biases diodes  $D_1$  and  $D_2$ . This applies voltage  $-V_g$  across the primary winding, thereby resetting the transformer. The duty cycle is again limited to  $D < 0.5$ . This converter has the advantage that the transistor peak blocking voltage is limited to  $V_g$ , and is clamped by diodes  $D_1$  and  $D_2$ . This circuit is quite popular in power supplies having 240 Vac inputs.

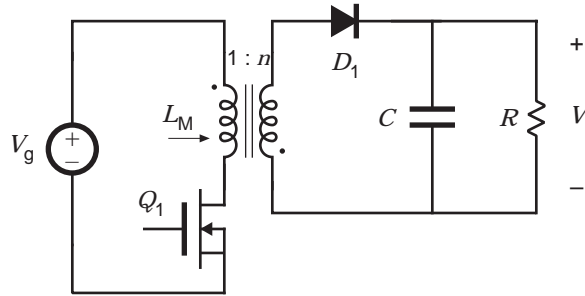


**Figure 13.** The flyback converter, a single-transistor isolated buck-boost converter.

### ***Flyback converter***

The flyback converter of Fig. 13 is based on the buck-boost converter. Although the two-winding magnetic device is represented using the same symbol as the transformer, a more descriptive name is “two-winding inductor.” This device is sometimes also called a “flyback transformer.” Unlike the ideal transformer, current does not flow simultaneously in both windings of the flyback transformer. Rather, the flyback transformer magnetizing inductance assumes the role of the inductor of the buck-boost converter. The magnetizing current is switched between the primary and secondary windings.

When transistor  $Q_1$  conducts, diode  $D_1$  is reverse-biased. The primary winding then functions as an inductor, connected to the input source  $V_g$ . Energy is stored in the magnetic field of the flyback transformer. When transistor  $Q_1$  turns off, the current ceases to flow in the primary winding. The magnetizing current, referred to the secondary winding, now forward-biases diode  $D_1$ . Energy stored in the magnetic field of the flyback transformer is then transferred to the dc load.

Application of the principle of inductor volt-second balance to the transformer primary winding leads to the following solution for the conversion ratio of the flyback converter:

$$M(D) = \frac{V}{V_g} = n \frac{D}{(1-D)} \quad (15)$$

Thus, the conversion ratio of the flyback converter is similar to that of the buck-boost converter, but with an added factor of  $n$ .

The flyback converter has traditionally been used in the high-voltage power supplies of televisions and computer monitors. It also finds widespread application in switching power supplies at the 50 W to 100 W power range. This converter has the advantage of very low parts count. Multiple outputs can be obtained using a minimum number of added elements: each auxiliary output requires only an additional winding, diode, and capacitor. However, in comparison with buck-derived transformer-isolated converters such as the full bridge and forward circuits, the flyback converter has the disadvantage of poor cross regulation.

### ***Switch implementation***

The switch network realization of Fig. 3 employs *single quadrant* switches. Each semiconductor element is able to conduct current of only one polarity in the on state, and block voltage of one polarity in the off state. This implies that, for proper functioning of the switch network, the source voltage, load

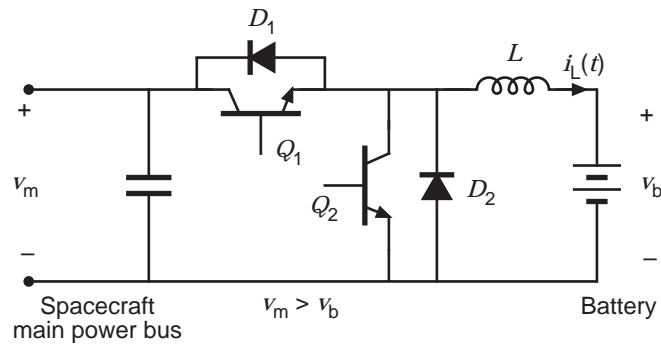


**Figure 14.** A buck converter with two-quadrant switches and bidirectional power flow. Spacecraft battery charger / discharger example.

voltage, and inductor current must all be positive. Consequently, the switch network allows the instantaneous power to flow in one direction only: from the source  $V_g$  towards to load.

Bidirectional (regenerative) power flow can be obtained with a current-bidirectional *two quadrant* realization of the switch network. An example is illustrated in Fig. 14, in which a dc-dc converter interfaces batteries to the main dc power bus of a spacecraft. The anti-parallel-connected transistors and diodes form current-bidirectional switches. Transistor  $Q_2$  is driven with the complement of the  $Q_1$  drive signal, such that  $Q_2$  is off when  $Q_1$  is on, and vice-versa. To charge the battery, the inductor current  $i_L(t)$  is positive and flows through transistor  $Q_1$  and diode  $D_2$ . To discharge the battery, the current  $i_L(t)$  reverses polarity, and flows through transistor  $Q_2$  and diode  $D_1$ . In both cases, the battery voltage is less than the main dc bus voltage. The magnitude and polarity of the battery current can be controlled via adjustment of the duty cycle  $D$ .

*Switching loss* imposes an upper limit on the switching frequencies of practical converters. During the switching transitions, the transistor voltage and current are simultaneously large. In consequence, the transistor experiences high instantaneous power loss. This can lead to significant average power loss, even though the switching transitions are short in duration. Switching loss causes the converter efficiency to decrease as the switching frequency is increased.

Several mechanisms lead to switching loss. Significant energy can be lost during the slow switching times of minority-carrier semiconductor devices such as BJTs, IGBTs, and thyristors. The diode reverse recovery process induces substantial additional energy loss in the transistor during the transistor turn-on transition. The energy stored in the semiconductor output capacitances is dissipated during the transistor turn-on transition. Energy stored in transformer leakage inductances and other stray inductances is usually dissipated by the transistor during the turn-off transition. The total switching loss is equal to the sum of the energy losses that arise via these mechanisms, multiplied by the switching frequency.

## Small-signal ac modeling

To design the control system of a converter, it is necessary to model the converter dynamic behavior. In particular, it is of interest to determine how variations in the power input voltage  $v_g(t)$ , the load current, and the duty cycle  $d(t)$  affect the output voltage. Unfortunately, understanding of converter dynamic behavior is hampered by the nonlinear time-varying nature of the switching and pulse-width modulation process. These difficulties can be overcome through the use of waveform averaging and small-signal modeling techniques [6-12]. A well-known converter modeling technique known as *state-space averaging* is briefly described here. Results for several basic converters are listed in tabular form.

### *State-space averaging*

The state-space averaging technique generates the low-frequency small-signal ac equations of PWM dc-dc converters. Converter transfer functions and equivalent circuit models can be obtained.

The converter contains independent state variables such as inductor currents and capacitor voltages, that form the state vector  $\mathbf{x}(t)$ , and the converter is driven by independent sources that form the input vector  $\mathbf{u}(t)$ . The output vector  $\mathbf{y}(t)$  contains dependent signals of interest. During the first subinterval, when the switches are in position 1 for time  $dT_s$ , the converter reduces to a linear circuit whose equations can be written in the following state-space form:

$$\begin{aligned}\frac{d\mathbf{x}(t)}{dt} &= \mathbf{A}_1\mathbf{x}(t) + \mathbf{B}_1\mathbf{u}(t) \\ \mathbf{y}(t) &= \mathbf{C}_1\mathbf{x}(t) + \mathbf{E}_1\mathbf{u}(t)\end{aligned}\quad (16)$$

The matrices  $\mathbf{A}_1$ ,  $\mathbf{B}_1$ ,  $\mathbf{C}_1$ , and  $\mathbf{E}_1$  describe the network connections during the first subinterval. The duty cycle  $d(t)$  may now be a time-varying quantity. During the second subinterval, the converter reduces to another linear circuit, whose state space equations are

$$\begin{aligned}\frac{d\mathbf{x}(t)}{dt} &= \mathbf{A}_2\mathbf{x}(t) + \mathbf{B}_2\mathbf{u}(t) \\ \mathbf{y}(t) &= \mathbf{C}_2\mathbf{x}(t) + \mathbf{E}_2\mathbf{u}(t)\end{aligned}\quad (17)$$

The matrices  $\mathbf{A}_2$ ,  $\mathbf{B}_2$ ,  $\mathbf{C}_2$ , and  $\mathbf{E}_2$  describe the network connections during the second subinterval, of length  $(1-d)T_s$ .

It is assumed that the natural frequencies of the converter network are much smaller than the switching frequency. This assumption coincides with the small ripple approximation, and is usually satisfied in well-designed converters. It allows the high-frequency switching harmonics to be removed by an averaging process. In addition, the waveforms are linearized about a dc quiescent operating point. The converter waveforms are expressed as quiescent values plus small ac variations, as follows:

$$\begin{aligned}\mathbf{x}(t) &= \mathbf{X} + \hat{\mathbf{x}}(t) \\ \mathbf{u}(t) &= \mathbf{U} + \hat{\mathbf{u}}(t) \\ \mathbf{y}(t) &= \mathbf{Y} + \hat{\mathbf{y}}(t) \\ d(t) &= D + \hat{d}(t)\end{aligned}\quad (18)$$

This small-signal linearization is justified provided that

$$\begin{aligned}
\|\mathbf{X}\| &\gg \|\hat{\mathbf{x}}(t)\| \\
\|\mathbf{U}\| &\gg \|\hat{\mathbf{u}}(t)\| \\
\|\mathbf{Y}\| &\gg \|\hat{\mathbf{y}}(t)\| \\
D &\gg |\hat{d}(t)|
\end{aligned} \tag{19}$$

where  $\|\mathbf{x}\|$  represents the norm of vector  $\mathbf{x}$ .

The state-space averaged model that describes the quiescent converter waveforms is

$$\begin{aligned}
\mathbf{0} &= \mathbf{A}\mathbf{X} + \mathbf{B}\mathbf{U} \\
\mathbf{Y} &= \mathbf{C}\mathbf{X} + \mathbf{E}\mathbf{U}
\end{aligned} \tag{20}$$

where the averaged state matrices are

$$\begin{aligned}
\mathbf{A} &= D\mathbf{A}_1 + (1-D)\mathbf{A}_2 \\
\mathbf{B} &= D\mathbf{B}_1 + (1-D)\mathbf{B}_2 \\
\mathbf{C} &= D\mathbf{C}_1 + (1-D)\mathbf{C}_2 \\
\mathbf{E} &= D\mathbf{E}_1 + (1-D)\mathbf{E}_2
\end{aligned} \tag{21}$$

The steady-state solution of the converter is

$$\begin{aligned}
\mathbf{X} &= -\mathbf{A}^{-1}\mathbf{B}\mathbf{U} \\
\mathbf{Y} &= \left(-\mathbf{C}\mathbf{A}^{-1}\mathbf{B} + \mathbf{E}\right)\mathbf{U}
\end{aligned} \tag{22}$$

The state equations of the small-signal ac model are

$$\begin{aligned}
\frac{d\hat{\mathbf{x}}(t)}{dt} &= \mathbf{A}\hat{\mathbf{x}}(t) + \mathbf{B}\hat{\mathbf{u}}(t) + \left[\left(\mathbf{A}_1 - \mathbf{A}_2\right)\mathbf{X} + \left(\mathbf{B}_1 - \mathbf{B}_2\right)\mathbf{U}\right]\hat{d}(t) \\
\hat{\mathbf{y}}(t) &= \mathbf{C}\hat{\mathbf{x}}(t) + \mathbf{E}\hat{\mathbf{u}}(t) + \left[\left(\mathbf{C}_1 - \mathbf{C}_2\right)\mathbf{X} + \left(\mathbf{E}_1 - \mathbf{E}_2\right)\mathbf{U}\right]\hat{d}(t)
\end{aligned} \tag{23}$$

These equations describe how small ac variations in the input vector and duty cycle excite variations in the state and output vectors.

### ***Canonical model***

Equivalent circuit models of dc-dc converters can be constructed using the state-space averaged equations (20) and (23). Since all PWM dc-dc converters perform similar basic functions, one finds that the equivalent circuit models have the same form. Consequently, the *canonical circuit model* of Fig. 15 can represent the physical properties of PWM dc-dc converters.

The primary function of a dc-dc converter is the transformation of dc voltage and current levels, ideally with 100% efficiency. This function is represented in the model by an ideal *dc transformer*, denoted by a transformer symbol having a solid horizontal line. The dc transformer model has an effective turns ratio equal to the quiescent conversion ratio  $M(D)$ . It obeys all of the usual properties of transformers, except that it can pass dc voltages and currents. Although conventional magnetic-core transformers cannot pass dc voltages, we are nonetheless free to define an ideal dc transformer symbol; use of this symbol in modeling dc-dc converter properties is justified because its predictions are correct.

Small ac variations in the source voltage  $v_g(t)$  are also transformed by the conversion ratio  $M(D)$ . Hence, a sinusoidal line is added to the dc transformer symbol, to denote that it also correctly represents how small-signal ac variations pass through the converter.

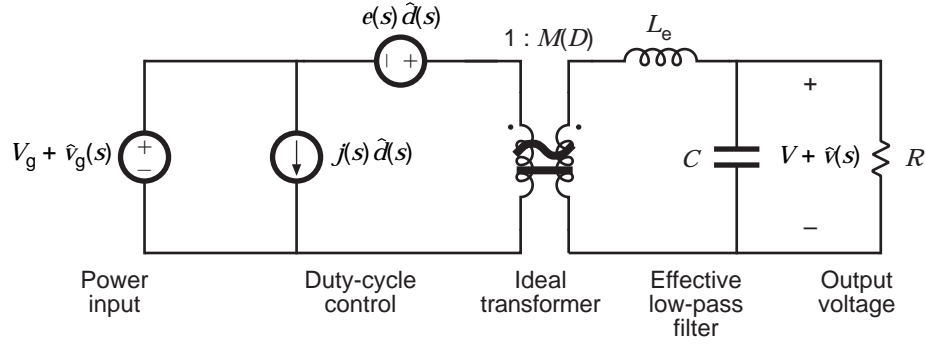


**Figure 15.** The canonical model: a small-signal equivalent circuit that models dc-dc converter dynamics and transfer functions.

Small ac variations in the duty cycle  $d(t)$  excite ac variations in the converter voltages and currents. This is modeled by the  $e(s)d$  and  $j(s)d$  generators of Fig. 15. In general, both a current source and a voltage source are required.

The converter inductors and capacitors, necessary to low-pass filter the switching harmonics, also low-pass filter ac variations. The canonical model therefore contains an effective low-pass filter. Figure 15 illustrates the two-pole low-pass filter of the buck, boost, and buck-boost converters; complex converters having additional inductors and capacitors, such as the Cuk and SEPIC, contain correspondingly complex effective low-pass filters. The element values in the effective low-pass filter do not necessarily coincide with the physical element values in the converter. In general, the element values, transfer function, and terminal impedances of the effective low-pass filter can vary with quiescent operating point.

Canonical model parameters for the ideal buck, boost, and buck-boost converters are listed in Table 1. Transformer isolated versions of the buck, boost, and buck-boost converters, such as the full bridge, forward, and flyback converters, can also be modeled using the equivalent circuit of Fig. 15 and the parameters of Table 1; one must then correctly account for the transformer turns ratio by referring all quantities to the transformer secondary.

**Table 1.** Canonical model parameters for several basic converters

Converter	$M(D)$	$L_e$	$e(s)$	$j(s)$
Buck	$D$	$L$	$\frac{V}{D^2}$	$\frac{V}{R}$
Boost	$\frac{1}{(1-D)}$	$\frac{L}{(1-D)^2}$	$V \left( 1 - \frac{sL}{(1-D)^2 R} \right)$	$\frac{V}{(1-D)^2 R}$
Buck-boost	$-\frac{D}{(1-D)}$	$\frac{L}{(1-D)^2}$	$-\frac{V}{D^2} \left( 1 - \frac{sDL}{(1-D)^2 R} \right)$	$-\frac{V}{(1-D)^2 R}$

### ***Small-signal transfer functions of the buck, boost, and buck-boost converters***

The canonical circuit model of Fig. 15 can be solved using conventional linear circuit analysis techniques, to find quantities of interest such as the small-signal control-to-output and line-to-output transfer functions. The control-to-output transfer function  $G_d(s)$  is the transfer function from  $d(s)$  to  $v(s)$ , with  $v_g(s)$  set to zero. The line-to-output transfer function  $G_g(s)$  is the transfer function from  $v_g(s)$  to  $v(s)$ , with  $d(s)$  set to zero. For the buck, boost, and buck-boost converters, these transfer functions can be written in the following forms

$$G_d(s) = G_{d0} \frac{\left(1 - \frac{s}{\omega_z}\right)}{1 + \frac{s}{Q\omega_0} + \left(\frac{s}{\omega_0}\right)^2} \quad (24)$$

$$G_g(s) = G_{g0} \frac{1}{1 + \frac{s}{Q\omega_0} + \left(\frac{s}{\omega_0}\right)^2} \quad (25)$$

Expressions for the parameters of Eqs. (24) and (25) are listed in Table 2. The boost and buck-boost converters exhibit control-to-output transfer functions containing two poles and one right half-plane (nonminimum phase) zero. The buck converter  $G_d(s)$  exhibits two poles but no zero. The line-to-output transfer functions of all three converters contain two poles and no zeroes.

The results of Table 2 can be applied to transformer-isolated versions of the buck, boost, and buck-boost converters, by referring all element values to the transformer secondary side. Equation (25) must also be multiplied by the transformer turns ratio.

The control systems of boost and buck-boost converters tend to be destabilized by the presence of the right-half plane (RHP) zero in the control-to-output transfer function. This occurs because, during a transient, the phase lag of the RHP zero causes the output to initially change in the wrong direction. When a RHP zero is present, it is difficult to obtain an adequate phase margin in conventional single-loop feedback systems having wide bandwidth. Prediction of the RHP zero, and the consequent explanation of why the feedback loops controlling continuous conduction mode boost and buck-boost converters tend to oscillate, was one of the early successes of averaged converter modeling and state-space averaging.

**Table 2** Small-signal transfer function parameters for basic dc-dc converters

Converter	$G_{g0}$	$G_{d0}$	$\omega_0$	$Q$	$\omega_z$
Buck	$D$	$\frac{V}{D}$	$\frac{1}{\sqrt{LC}}$	$R\sqrt{\frac{C}{L}}$	$\infty$
Boost	$\frac{1}{(1-D)}$	$\frac{V}{(1-D)}$	$\frac{(1-D)}{\sqrt{LC}}$	$(1-D)R\sqrt{\frac{C}{L}}$	$\frac{(1-D)^2 R}{L}$
Buck-Boost	$-\frac{D}{(1-D)}$	$\frac{V}{D(1-D)^2}$	$\frac{(1-D)}{\sqrt{LC}}$	$(1-D)R\sqrt{\frac{C}{L}}$	$\frac{(1-D)^2 R}{DL}$

## BIBLIOGRAPHY

1. R. D. Middlebrook, Power electronics: topologies, modeling, and measurement, *Proc. IEEE Int. Symp. Circuits Syst.*, April 1981.
2. S. Cuk, Basics of switched-mode power conversion: topologies, magnetics, and control, in *Advances in Switched-Mode Power Conversion*, vol. 2, pp. 279-310, Irvine: Teslaco, 1981.
3. R. W. Erickson, *Fundamentals of Power Electronics*, New York: Chapman and Hall, 1997.
4. R. Severns and G. E. Bloom, *Modern Dc-to-Dc Switchmode Power Converter Circuits*, New York: Van Nostrand Reinhold, 1985.
5. N. Mohan, T. Undeland, and W. Robbins, *Power Electronics: Converters, Applications, and Design*, 2nd ed., New York: John Wiley & Sons, 1995.
6. R. D. Middlebrook and S. Cuk, A general unified approach to modeling switching-converter power stages," *Int. J. Electronics*, vol. 42, no. 6, pp. 521-550, June 1977.
7. S. Cuk, Modeling, analysis, and design of switching converters," Ph.D. thesis, California Institute of Technology, November 1976.
8. G. W. Wester and R. D. Middlebrook, Low frequency characterization of switched dc-dc converters, *IEEE Trans. Aerosp. Electron. Syst.*, vol. AES-9, pp. 376-385, May 1973.
9. D. M. Mitchell, *Dc-Dc Switching Regulator Analysis*, New York: McGraw-Hill, 1988.
10. P. T. Krein, J. Bentsman, R. M. Bass, and B. C. Lesieutre, On the use of averaging for the analysis of power electronic systems," *IEEE Trans. Power Electron.*, vol. 5, no. 2, pp. 182-190, April 1990.
11. A. Kislovski, R. Redl, and N. Sokal, *Dynamic Analysis of Switching-Mode DC/DC Converters*, New York: Van Nostrand Reinhold, 1994.
12. V. Vorperian, R. Tymerski, and F. C. Lee, Equivalent circuit models for resonant and PWM switches, *IEEE Trans. Power Electron.*, vol. 4, no. 2, pp. 205-214, April 1989.